Morphology Tailoring of Thin Film Block Copolymers on Patterned Substrates

Xianggui Ye, Brian J. Edwards, Bamin Khomami*

It is well known that chemically patterned substrates can direct the assembly of adsorbed layers or thin films of block copolymers. For a cylinder-forming diblock copolymer on periodically spot-patterned substrates, the morphology of the block copolymer follows the pattern at the substrate; however, with different periodic spacing and spot size of the pattern, novel morphologies can be created. Specifically, we have demonstrated that new morphologies that are absent in the bulk system can be tailored by judiciously varying the mismatch between the width of the pattern and the periodic spacing of the bulk block copolymer, the top surface affinity, and spot size. New morphologies can thus be achieved, such as honeycomb and ring structures, which do not appear in the bulk system. These results demonstrate a promising strategy for fabrication of new nanostructures from chemically patterned substrates.

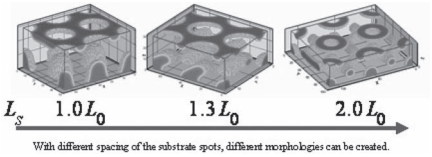

With different spacing of the substrate spots, different morphologies can be created.

1. Introduction

Block copolymers (BCPs) are composed of two or more chemically distinct and frequently immiscible blocks that are covalently bonded to each other. Because of thermodynamic incompatibility, distinct blocks will self-organize into different microstructures via microphase separation. This unique property of BCPs has been explored in many potential applications, including nanostructured membranes, BCP templates for nanoparticle synthesis, photonic crystals, and high-density information storage media.[1–3] The precise control of BCP microdomain patterns over a long length scale is very challenging but of upmost importance in the aforementioned applications. Hence, many research groups have had their focus on development of techniques to create long-range order in BCPs. Currently, two main techniques are primarily being used for producing morphologies with long-range order. The first method utilizes nonequilibrium processes, such as solvent evaporation, or use of an external field, and the second technique relies on substrates with topographic or chemical patterns.[4–11]

To date, the aforementioned techniques have been successfully used to achieve long-range ordered morphologies obtained in bulk systems.[4–9] However, a few recent studies have focused their attention on the use of chemically patterned substrates to create new morphologies that cannot be created in bulk BCP systems.[12–15] One example is where lamellae-forming block copolymer materials on square spotted chemical patterns form "quadratically perforated lamellae" morphologies.[12] Another is a mixed morphology of parallel half-cylinders on preferential stripes and perpendicular cylinders on neutral stripes, which is obtained from directed assembly of block copolymers on incompatible surface patterns.[13] More Recently, Daoulas et al.[14] have used directed assembly of supramolecular copolymers in thin films on chemically patterned substrates for creating device-oriented nanostructures that cannot be obtained in bulk system.[14] In addition, we have recently demonstrated that under confinement (thin film between two surfaces) that by changing the periodicity of stripe-patterns the bulk lamella structure can be converted to a bilamellar structure with different orientation, or a bilamellar structure with the same orientation.[15]

Dr. X. Ye, Prof. B. J. Edwards, Prof. B. Khomami
Materials Research and Innovation Laboratory,
Department of Chemical and Biomolecular Engineering,
University of Tennessee, Knoxville, TN 37996, USA
E-mail: bkhomami@utk.edu
Dr. X. Ye, Prof. B. J. Edwards, Prof. B. Khomami
Sustainable Energy Education and Research Center,
University of Tennessee, Knoxville, TN 37996, USA

DOI: 10.1002/marc.201100744

As demonstrated by these and other studies,[16,17] confinement in general can be used to create new morphologies due to interfacial interactions, symmetry breaking, structural frustration, and confinement-induced entropy loss. In this work, we have examined morphological transition in BCPs under confinement between a chemically spot-patterned surface and a homogeneous surface. Specifically, the influence of the spot spacing, size of the spot, and the homogeneous surface affinity effect on the morphological transition are elucidated.

2. Results and Discussion

Self-consistent field theory (SCFT) has proven to be one of the most successful theoretical methods for investigating equilibrium phases in BCPs and has played a major role in establishing the phase diagram of bulk block copolymer melts.[18,19] The free energy of the system is expressed as

$$F/nk_BT = -\ln(Q_p/V) + \frac{1}{V}\int d\mathbf{r}[\chi_{AB}N\phi_A(\mathbf{r})\phi_B(\mathbf{r}) - w_A(\mathbf{r})\phi_A(\mathbf{r}) - w_B(\mathbf{r})\phi_B(\mathbf{r}) + H(\mathbf{r})(\phi_A(\mathbf{r}) - \phi_B(\mathbf{r})) - P(\mathbf{r})(1 - \phi_A(\mathbf{r}) - \phi_B(\mathbf{r}))] \quad (1)$$

where $H(\mathbf{r})$ is the polymer–surface interaction, which is assumed to be short-ranged, and which has the same units as the Flory-Huggins interaction parameter, χ_{AB}. Note that *A* and *B* refer to different blocks of the BCP. Specifically, when the simulation cells are adjacent to the patterned surface, $H(\mathbf{r}) = H_A$ or H_B; otherwise, $H(\mathbf{r}) = 0$, and the strength of a lattice relative to the pattern surface; (i.e., H_A and H_B) depends on the patterned surface. When $H(\mathbf{r})$ is negative, the surface favors A segments, and when $H(\mathbf{r})$ is positive, it favors B segments. $w_A(\mathbf{r})$ and $w_B(\mathbf{r})$ are the mean fields, which are produced by the surrounding chains. $P(\mathbf{r})$ is a Lagrange multiplier (in the form of a pressure) that is used to ensure that the incompressibility condition is satisfied. The magnitude of *H* is 7, and *H* is positive in the white region, and *H* is negative in the red region (see Figure 1). No significant difference has been found when the magnitude of H is 3.5. The range of H values used in this study has been motivated by earlier studies of the PS-PMMA BCP.[20] More details regarding the computations can be found in our previous publication.[15] For an asymmetric diblock copolymer $f_A = 0.30$ (volume fraction of block A) at $\chi_{AB}N = 20.0$, the bulk cylinder spacing is $L_o = 4.19\ R_g$. and the radius of a cylinder is 1.12 R_g. For $\chi_{AB}N = 20.0$, the phase behavior relates behaviors for intermediate-segregation region BCPs, which is experimentally more relevant.[19] Also, in this regime, neither the strong-segregation theory[21] nor the weak-segregation theory of Leibler[22] provides an adequate description of phase behavior of this region. In this study, relatively thin films of thickness of approximately 4.42 R_g have been studied.

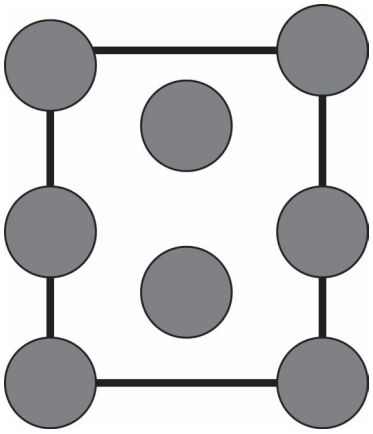

Figure 1. Schematic illustration of the bottom surface. The white region attracts A-blocks, and the red region attracts B-blocks.

Experimentally, the interaction between the polymer and the surface can be tuned by the surface chemistry.[20,23] Specifically, one way to change the surface affinity is to modify the surface using a polymer brush.[20] Recently, Albert et al.[23] created a gradient with chemical functionalities that mimics the structures of PS and PMMA, and demonstrated the utility of the fabricated gradient in a PS-*b*-PMMA thin film morphology study in which they identified the expected morphological changes across the gradient. Another approach to tune surface affinity is based on the use of different solvent vapor treatments.[24–27] It should be noted that, experimentally, the top surface is usually a free surface, which may play an important role in morphology formation.[28,29] However, in this study, we focus our attention on the morphology formation between two solid surfaces; that is, one is homogeneous, and the other is chemically patterned.

The top surface affinity for the longer block of the diblock copolymer plays a critical role in determining the thin film morphology (see Figure 2). It should be noted that the bottom dotted patterned surface is kept unchanged in the computed morphologies depicted in Figure 2. Clearly, for the top row of morphologies, in the middle of the film, the minor block of the diblock copolymer forms a honeycomb network structure, which may have many potential applications.[1] However, the bottom morphology is similar to a vertical cylinder morphology.

The specific affinity of the top surface for the longer block of the diblock copolymer can alter the stability of the resulting morphologies due to small free energy differences in particular morphologies of the BCP.[30] Obviously (see Figure 2), when the top surface is neutral to segments *A* and *B*, the vertical cylinder morphology is more stable, as determined experimentally.[5,10] As the top surface affinity for the longer block is increased, the

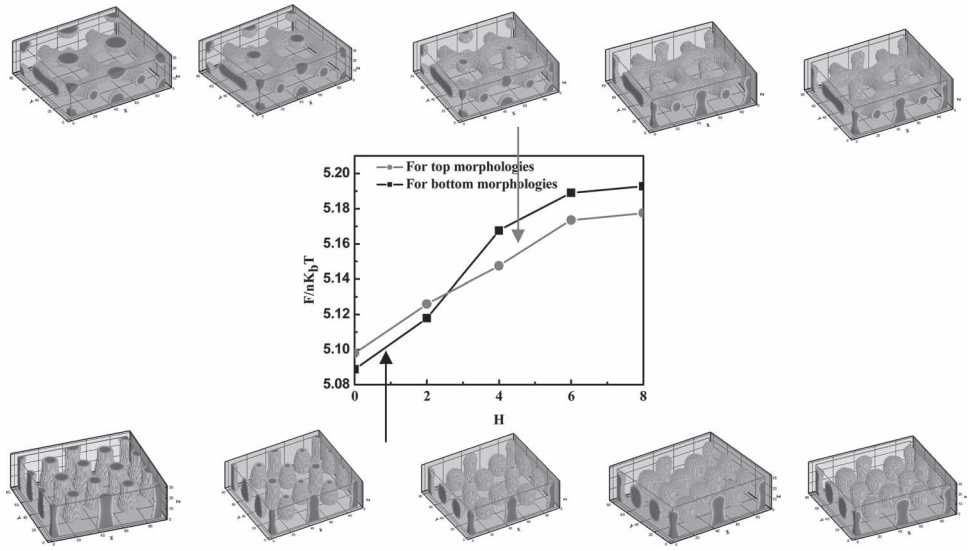

Figure 2. Free energy per chain as a function of the top surface affinity for the longer block of diblock copolymer. The solid dots and the solid squares indicate the free energies of top morphologies and the bottom morphologies, respectively. The thickness of the film is 4.42 R_g. The spacing period of the spot pattern is 1.6 L_o and the dot size is 1.12 R_g.

free energy difference between the top and bottom morphologies depicted in Figure 2 decreases. Specifically, at H of approximately 3.0, the top morphologies with the honeycomb structure become more stable.

The spacing of the spots and spot size also has a significant effect on the morphology of the BCP in thin films. Figure 3 shows the morphologies with three different spacing periods and two different dot sizes. To focus on the effect of dot spacing period and dot size on the morphology, the top surface is kept neutral to segment A and segment B, that is, H = 0.0. The enrichment of the shorter block of the BCP is observed at the top surface due to reduced entropic loss when the shorter block is closer to the surface.[31] Two dot sizes have been studied. In one case, the radius of the spots is 0.88 R_g, which is 21% smaller than that of cylinder size of the BCP in bulk. The other radius of the spots is 1.47 R_g, which is 31% larger than that of cylinder size of the BCP in bulk.

When the spacing of the dots is commensurate with that of the cylinders in bulk; that is, $L_s = L_0$, the vertical cylinder-like structures are found for the two systems with different dot sizes close to the bottom surface (see left column in Figure 3). For the smaller dot size system, the size of the cylinders increases with distance from the bottom surface initially, and then decrease quickly; however, for the larger dot size system, the size of the cylinders decreases with distance

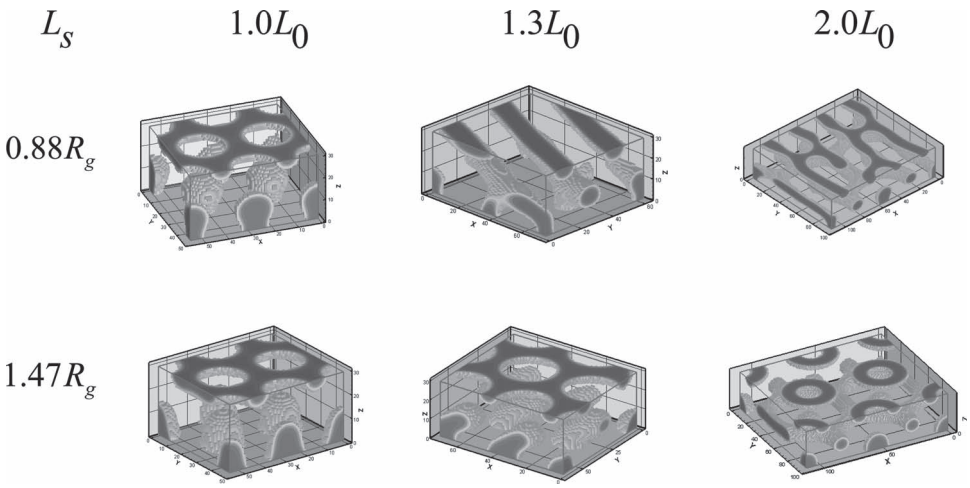

Figure 3. Morphological transition as a function of spot spacing and dot size. The first column, the second column, and the third column are for dot spacing of, 1.0 L_o, 1.3 L_o, and 2.0 L_o, respectively. The first and the second row of the morphologies are for dot sizes, 0.88 R_g, and 1.47 R_g, respectively.

from the bottom surface. Close to the top surface, the honeycomb structure is observed for both systems, in which the minor component of the diblock copolymer forms the honeycomb network structure.

When the spacing of the dots increases to $L_s = 1.3L_0$, different morphologies have been obtained with different dot sizes (see middle column in Figure 3). For the smaller dot size system, parallel cylinders have been formed close to the patterned surface. However, for the larger dot size system, the tilt cylinder morphology exists near the bottom surface, and the honeycomb structure is observed near the top surface. Increasing the spacing of the dots to $L_s = 2.0L_0$, also results in different morphologies (see right column in Figure 3). For the dot size of 0.88 R_g, the parallel cylinders are formed close to the patterned surface, similar to that of $L_s = 1.3L_0$. However, for the dot size of 1.47 R_g, a complicated structure is observed as shown at the bottom right of Figure 3. Close to the top surface, a ring structure is observed. Such a morphology has previously been found in nanopore confinement.[16,17] However, the ring structure is not formed in the confinement direction. In the middle of the thin film, the honeycomb structure is again observed.

3. Conclusion

In summary, chemically patterned substrates can direct the assembly of adsorbed layers or thin films of block copolymers. For a cylinder-forming diblock copolymer on periodically spot-patterned substrates, the morphology of the block copolymer follows the pattern at the substrate; however, a host of novel morphologies can be created via judicious manipulation of periodic spacing and dot size of the spot pattern. Specifically, by tuning the top surface affinity to the longer block of the BCP and the spot size at the bottom surface, thin films can attain novel morphologies that are entirely absent in the bulk system. Therefore, in addition to tuning the architecture of the block copolymer, there are three other parameters that can be used to influence the morphology in thin films of block copolymers; namely, mismatch between the width of the spot pattern and the periodic spacing of the bulk block copolymer, the top surface affinity, and the spot size on the bottom surface.[32–34] These results demonstrate a promising strategy for fabrication of new nanostructures from chemically patterned substrates.

Acknowledgements: Funding for this project was provided by the Sustainable Energy Education and Research Center at the University of Tennessee-Knoxville. B.K. would like to acknowledge NSF for partial support this work, CBET-0932666.

Received: November 7, 2011; Revised: December 8, 2011; Published online: January 30, 2012; DOI: 10.1002/marc.201100744

Keywords: block copolymers; confinement; directed self-assembly; microphase separation; microstructure; self-consistent field theory

[1] C. Park, J. Yoon, E. L. Thomas, *Polymer* **2003**, *44*, 6725.
[2] S. B. Darling, *Prog. Polym. Sci.* **2007**, *32*, 1152.
[3] I. W. Hamley, *Prog. Polym. Sci.* **2009**, *34*, 1161.
[4] M. P. Stoykovich, M. Muller, S. O. Kim, H. H. Solak, E. W. Edwards, J. J. de Pablo, P. F. Nealey, *Science* **2005**, *308*, 1442.
[5] R. Ruiz, H. M. Kang, F. A. Detcheverry, E. Dobisz, D. S. Kercher, T. R. Albrecht, J. J. de Pablo, P. F. Nealey, *Science* **2008**, *321*, 936.
[6] G. W. Peng, F. Qiu, V. V. Ginzburg, D. Jasnow, A. C. Balazs, *Science* **2000**, *288*, 1802.
[7] S. H. Kim, M. J. Misner, T. Xu, M. Kimura, T. P. Russell, *Adv. Mater.* **2004**, *16*, 226.
[8] Z. Q. Lin, D. H. Kim, X. D. Wu, L. Boosahda, D. Stone, L. LaRose, T. P. Russell, *Adv. Mater.* **2002**, *14*, 1373.
[9] F. A. Detcheverry, P. F. Nealey, J. J. de Pablo, *Macromolecules* **2010**, *43*, 6495.
[10] R. A. Segalman, *Science* **2008**, *321*, 919.
[11] R. A. Segalman, A. Hexemer, E. J. Kramer, *Macromolecules* **2003**, *36*, 6831.
[12] K. C. Daoulas, M. Muller, M. P. Stoykovich, S. M. Park, Y. J. Papakonstantopoulos, J. J. de Pablo, P. F. Nealey, H. H. Solak, *Phys. Rev. Lett.* **2006**, *96*, 036104.
[13] S. O. Kim, B. H. Kim, D. Meng, D. O. Shin, C. M. Koo, H. H. Solak, Q. Wang, *Adv. Mater.* **2007**, *19*, 3271.
[14] K. C. Daoulas, A. Cavallo, R. Shenhar, M. Muller, *Phys. Rev. Lett.* **2010**, *105*, 108301.
[15] X. G. Ye, B. J. Edwards, B. Khomami, *Macromolecules* **2010**, *43*, 9594.
[16] Y. Y. Wu, G. S. Cheng, K. Katsov, S. W. Sides, J. F. Wang, J. Tang, G. H. Fredrickson, M. Moskovits, G. D. Stucky, *Nat. Mater.* **2004**, *3*, 816.
[17] B. Yu, P. Sun, T. Chen, Q. Jin, D. Ding, B. Li, A.-C. Shi, *Phys. Rev. Lett.* **2006**, *96*, 138306.
[18] F. Drolet, G. H. Fredrickson, *Phys. Rev. Lett.* **1999**, *83*, 4317.
[19] M. W. Matsen, F. S. Bates, *J. Chem. Phys.* **1997**, *106*, 2436.
[20] F. A. Detcheverry, G. L. Liu, P. F. Nealey, J. J. de Pablo, *Macromolecules* **2010**, *43*, 3446.
[21] A. N. Semenov, *Macromolecules* **1989**, *22*, 2849.
[22] L. Leibler, *Macromolecules* **1980**, *13*, 1602.
[23] J. N. L. Albert, M. J. Baney, C. M. Stafford, J. Y. Kelly, T. H. Epps, *Acs Nano* **2009**, *3*, 3977.
[24] J. N. L. Albert, T. D. Bogart, R. L. Lewis, K. L. Beers, M. J. Fasolka, J. B. Hutchison, B. D. Vogt, T. H. Epps, *Nano Lett.* **2011**, *11*, 1351.
[25] K. A. Cavicchi, K. J. Berthiaume, T. P. Russell, *Polymer* **2005**, *46*, 11635.
[26] J. G. Son, A. F. Hannon, K. W. Gotrik, A. Alexander-Katz, C. A. Ross, *Adv. Mater.* **2011**, *23*, 634.
[27] J. K. Bosworth, M. Y. Paik, R. Ruiz, E. L. Schwartz, J. Q. Huang, A. W. Ko, D. M. Smilgies, C. T. Black, C. K. Ober, *ACS Nano* **2008**, *2*, 1396.
[28] C. Forrey, K. G. Yager, S. P. Broadaway, *Acs Nano* **2011**, *5*, 2895.
[29] S. M. Park, B. C. Berry, E. Dobisz, H. C. Kim, *Soft Matter* **2009**, *5*, 957.
[30] M. Muller, K. C. Daoulas, Y. Norizoe, *Phys. Chem. Chem. Phys.* **2009**, *11*, 2087.
[31] M. W. Matsen, *Macromolecules* **2010**, *43*, 1671.
[32] X. G. Ye, T. F. Shi, Z. Y. Lu, C. X. Zhang, Z. Y. Sun, L. J. An, *Macromolecules* **2005**, *38*, 8853.
[33] X. G. Ye, X. F. Yu, T. F. Shi, Z. Y. Sun, L. J. An, Z. Tong, *J. Phys. Chem. B* **2006**, *110*, 23578.
[34] X. G. Ye, X. F. Yu, Z. Y. Sun, L. J. An, *J. Phys. Chem. B* **2006**, *110*, 12042.